The dependence of initial states on the excitation of NO molecules by chirped infrared laser pulses

2000 J. Phys. B: At. Mol. Opt. Phys. 33 3023

(http://iopscience.iop.org/0953-4075/33/16/307)

J. Phys. B: At. Mol. Opt. Phys. **33** (2000) 3023–3036. Printed in the UK PII: S0953-4075(00)50487-8

The dependence of initial states on the excitation of NO molecules by chirped infrared laser pulses

J T Lin† and T F Jiang‡

† National Center for Theoretical Sciences, Physics Division, PO Box 2-131, Hsinchu 30013, Taiwan

‡ Institute of Physics, National Chiao Tung University, Hsinchu 30010, Taiwan

Received 6 April 2000, in final form 5 June 2000

Abstract. We study the effect of initial states on the chirping excitation of NO molecules in order to interpret recent experimental data. The results show that excitation is efficient when the probability density localizes along the polarization direction of the external field. Therefore, the thermal effect on the density distribution must be taken into account for the experimental case of 15 K. Furthermore, as the adiabatic limit is fully satisfied, the interference pattern of excited state populations disappears. This becomes a limiting factor under experimental conditions. We also find that excitation can be enhanced significantly when the pulse intensity is increased to fit the adiabatic criterion.

1. Introduction

The control of molecular dynamics and its reaction yields by lasers have been investigated extensively over the last two decades. Among the various approaches that have been proposed [1–24], of particular interest is that based on multiphoton vibrational excitation and the dissociation of molecules by intense, infrared laser pulses adapted appropriately to the inherent molecular structure [3, 25, 26]. One might expect the laser to selectively excite or break a particular molecular bond rapidly, resulting in a chemical reaction on a time scale which is shorter than the various relaxation time scales in the molecular medium. However, this kind of multiphoton process is difficult to achieve using monochromatic infrared pulses for two reasons. First, the population transfer between two neighbouring vibrational states is small because of the small transition moment. High-intensity lasers can increase the transition efficiency of low-lying states to that of the high-vibrational states. However, the molecular dissociation is then overwhelmed by atomic ionization and rapid monochromatic excitation is limited by such destructive processes in the mean time [27, 28]. Secondly, the anharmonicity of molecular vibrations is responsible for this difficulty of sequential transitions among the molecular ladder climbing. If the laser frequency is tuned to optimize the first vibrational transition, the second transition will be out of resonance and the population inversion will be reduced dramatically.

Several methods of increasing the vibrational excitation rates have been suggested, such as using modulated amplitude or phase pulses, or irradiating molecules with a train of optimal pulses [1, 5, 26, 29–32]. As suggested by Chelkowski and co-workers [2–4], vibrational excitation will increase significantly if the laser frequency is tuned to the subsequent transition frequencies when the inversion in the previous transition is already accomplished. This specific

0953-4075/00/163023+14$30.00

frequency-sweeping (chirping) pulse provides a more robust method of population transfer (adiabatic passage) than other methods on a time scale which is shorter than the relaxation time [2, 33]. However, although these specific chirped pulses are optimal for the molecular structure, it is hard, in practice, to construct such pulses. It has been shown that linear chirped pulses can also achieve almost the same vibrational excitation and dissociation of diatomic molecules as the optimal chirped pulses [13–16]. Furthermore, interference in the vibrational ladder will make the excitation complicated and impose additional constraint on the transition efficiency. Lin and Jiang [14] demonstrated excitation interference for the one-dimensional (1D) HF molecule versus chirping parameters and field strength in both the classical and quantum calculation without the rotational degree of freedom. This interference is mainly due to the competition between non-resonant multiphoton excitation and resonant multi-step excitation, which has been explored experimentally for rubidium atoms by Balling *et al* [17]. Recently, Maas *et al* [18, 19] performed some NO molecular chirping excitation experiments and investigated the rotational interference in the vibrational ladder climbing using a three-level model. This rotational interference is more important in a molecular system than the earlier competitive mechanism in the rubidium atom experiment [17] and in one-dimensional molecular systems [13, 14]. It also demonstrated that the oscillatory behaviour in the excited populations of NO molecules is not as clear as in the rubidium case for the chirping parameters used in these experiments. Therefore, it is interesting to explore the possible factors which lead to the vagueness of the beat pattern.

There has been little discussion about the effects of initial states and the intrapulse pump–dump process on *chirping excitation* [4, 8]. Consequently, our work will focus on these two themes. The paper is organized as follows. In section 2 we briefly describe our numerical method of full dimensional time-dependent calculation and the relationship between intensity and chirping which puts constraints on the adiabatic passage. Results and discussions are presented in section 3. We examine the chirping excitation of NO molecules by infrared lasers of different pulse intensities. The NO molecules are prepared in different initial states. Since the interference decreases as the transitions approach being fully adiabatic or diabatic, it is worthwhile studying the effect of intensities on the population transfer. We also include the thermal distribution of initial states in the population-transfer calculation and compare the results with experimental data and our previous calculated results [12]. Finally, a summary is given in section 4.

2. The numerical method: the split-operator algorithm

Under the Born–Oppenheimer approximation, the rovibrational states $|\phi_{v,l}\rangle$ in the ground electronic state can be described by the solution of the Hamiltonian

$$\hat{H}_0 = \frac{-\partial^2}{2\mu_m \partial R^2} + \frac{\hat{L}^2}{2\mu_m R^2} + D_e\left[1 - \mathrm{e}^{-\beta(R-R_0)}\right]^2. \tag{1}$$

To model the NO molecule, the potential parameters $D_e = 0.2388$, $\beta = 1.4648$, $\mu_m = 13\,709.9499$ and $R_0 = 2.175$ au are used. Here R denotes the relative coordinate of the atomic nuclei and μ_m represents the reduced mass of atoms N and O [15, 16]. Atomic units are used hereafter unless stated otherwise. Omitting the rotational term $\hat{L}^2/2\mu_m R^2$ reduces the system to a 1D model. In addition, the unperturbed Hamiltonian supports 55 vibrational bound states and rotational levels are associated with each vibrational state. The electric field of the chirped pulse can be expressed as

$$\boldsymbol{E}(t) = E_m \boldsymbol{e}_z \tfrac{1}{2}[\exp(-\Gamma t^2)\exp(\mathrm{i}\phi(t)) + \mathrm{c.c.}] \tag{2}$$

where $\phi(t) = \int_{-\infty}^{t} \omega(t')\,\mathrm{d}t'$ is the phase of the pulse at time t with chirped frequency $\omega(t)$. The light pulse is chirped by passing it through a pulse shaper which is centred around ω_0 with a small bandwidth $\Delta\omega$ and duration τ_0 [18, 34]. The output light is then composed of the different phase delay components with a new bandwidth parameter [36]

$$\Gamma = \frac{\ln 2/\Delta\omega^2}{8[\ln 2/\Delta\omega^2]^2 + 2\alpha^2} \tag{3}$$

and a stretched pulse duration τ

$$\tau^2 = {\tau_0}^2 + \left[\frac{8\alpha \ln 2}{\tau_0}\right]^2 \tag{4}$$

where the α is the chirping parameter and is determined by the experimental conditions. If $\alpha \gg {\tau_0}^2$, the instantaneous frequency changes linearly in time during the pulse, with the rate of change $\mathrm{d}\omega/\mathrm{d}t$ being approximately inversely proportional to the chirping parameter α:

$$\omega(t) = \omega_0 + \frac{\alpha[\Delta\omega^2/\ln 2]^2}{8 + 2\alpha^2[\Delta\omega^2/\ln 2]^2}t. \tag{5}$$

In the case of adiabatic passage, $\mathrm{d}\omega/\mathrm{d}t (\approx 1/2\alpha)$ and $E_m (\propto \sqrt{\tau_0/\tau})$ decrease as α increases. Therefore, these two parameters compete with each other on both sides of the adiabatic criterion $\mathrm{d}\omega/\mathrm{d}t \ll \Omega_{\mathrm{Rabi}}^2$ which is often violated in our present calculation and where $\Omega_{\mathrm{Rabi}} = \sqrt{\Omega(t)^2 + \Delta(t)^2}$ is the Rabi frequency, $\Omega(t) = (2d_{l',l}E(t)/\hbar)\langle\nu'|\mu(R)|\nu\rangle$ and $\Delta(t)$ is the detuning of the carrier frequency from the transition frequency. $\mu(R)$ is the dipole moment and $d_{l',l}$ is equal to

$$\langle Y_{l',m}|\cos\theta|Y_{l,m}\rangle = [(l^2 - m^2)/(2l+1)(2l-1)]^{1/2}\delta_{l',l-1} + [({l'}^2 - m^2)/(2l'+1)(2l'-1)]^{1/2}\delta_{l'-1,l}.$$

For the electric field linearly polarized along the z-direction, the time-dependent Schrödinger equation (TDSE) is

$$\mathrm{i}\hbar\frac{\partial}{\partial t}|\Psi\rangle = \left\{\frac{\hat{\boldsymbol{P}}^2}{2\mu_m} + \hat{V}_l(R) - \boldsymbol{E}(t)\cdot\vec{\mu}(R)\right\}|\Psi\rangle \tag{6}$$

where the effective potential

$$\hat{V}_l(R) = D_e[1 - \mathrm{e}^{-\alpha_M(R-R_0)}]^2 + l(l+1)/(2\mu R^2)$$

and

$$\mu(R) = (p_a R^2 + p_b R + p_c)\exp[-p_d(R - p_e)^2]$$

$$p_a = 0.2772 \qquad p_b = -0.6426 \qquad p_c = -4.9012 \times 10^{-7}$$

$$p_d = 0.5363 \qquad p_e = 1.6462$$

which is fitted to the *ab initio* calculation results of the $^2\Pi$–$^2\Pi$ transition dipole moment [35]. In fact, the ground state doublet X $^2\Pi_{1/2}$ and X $^2\Pi_{3/2}$ are split by 119 cm^{-1} due to spin–orbit interaction. This open-shell property makes the dipole moment and transition more complicated than the closed-shell cases. However, the spin is conserved during the excitation process so that only the integral angular moments l are involved in the calculation. It is not difficult to identify the spectra using current experimental techniques. We will focus our calculation on the X $^2\Pi_{1/2}$ state only.

The above time-dependent system is propagated by the split-operator algorithm [37]. The wavefunction is expanded into partial waves:

$$\Psi(R, \Omega; t) = \sum_{l=0}^{l_{\max}} F_l(R; t) Y_{l,m}(\Omega). \tag{7}$$

The kinetic propagation of the radial wavefunction is accomplished by the fast Fourier transform method between coordinate and momentum spaces at each time step Δ [38]. For the linearly polarized field, the azimuthal quantum number m is conserved and hence the system is actually two dimensional. In addition, the propagation of the dipole coupling term can be solved analytically. We can write the angular coupling in terms of the spherical Bessel function and expand the product of the wavefunction and this coupling term as follows:

$$\mathrm{e}^{\pm \mathrm{i} k\mu(R)\cos\theta}\Psi(R, \Omega; t) = \sum_{l=0}^{l_{\max}} G_l(R; t) Y_{l,m}(\Omega). \tag{8}$$

Then, the time-dependent radial part becomes

$$G_{l'}(R; t) = \sum_{n=|l-l'|}^{n=l+l'} \sum_{l=0}^{l_{\max}} (-1)^m (\pm\mathrm{i})^n (2n+1)\sqrt{(2l+1)(2l'+1)}\, j_n(k\mu)$$
$$\times F_l(R; t)(-1)^{2(l'-n)-m}(2l+1)^{-1/2}\langle l'0; n0|l0\rangle\langle l'-m; n0|l-m\rangle \tag{9}$$

where $\langle l_1 m_1 l_2 m_2 | l_3 m_3\rangle$ is the Clebsch–Gordan coefficient, $\Omega = (\theta, \phi)$, $k = |E(t + \frac{1}{2}\Delta)|\Delta$ and $j_n(k\mu)$ is the spherical Bessel function of order n.

In the numerical calculation, the corresponding experimental parameters are followed. The NO molecules are irradiated by the (sub)picosecond chirped pulse with intensity $I_{\text{chirp}} = E_m^2$. Assume there is no energy loss before or after chirping, the output pulse has a field strength $E_m = \sqrt{I_{\max}\tau_0/\tau}$, which is smaller than the input pulse field strength due to the stretched duration, and the input pulse intensity $I_{\max} = 10^{10}$ W cm^{-2}. The infrared laser frequency is 1850 cm^{-1} with a bandwidth limit of 40 cm^{-1} [18]. In our calculation, the wavefunctions are sampled in a grid of 2048 points extending to 48 au, and 10–15 partial waves are used in the angular expansion. The population of the highest angular momentum partial wave is less than 10^{-14} at the end of propagation. In the field-free calibration, the norm of the wavefunction is accurate to the tenth decimal place during a propagation time of 0.37 ps. This ensures the reliability of our presentation of small probability.

The population probability of the νth state, $P_\nu(t)$, is defined as

$$P_\nu(t) \equiv \sum_{l=0}^{l_{\max}} P_{\nu,l}(t) \tag{10}$$

where $P_{\nu,l}(t) = |\langle\phi_{\nu,l}(t)|\Psi(t)\rangle|^2$ denotes the population of the lth rotational level of the νth vibrational state at time t and $\nu = 0, 1, 2, \ldots, 54$.

3. Results and discussions

3.1. The effect of initial states on the population excitation

It has been shown that the accessible excitation pathways have a great influence on the population transfer [17, 18, 20]. It is, therefore, intriguing to examine the dependence of excitation on the initial states. We calculate the populations to the first and third excited

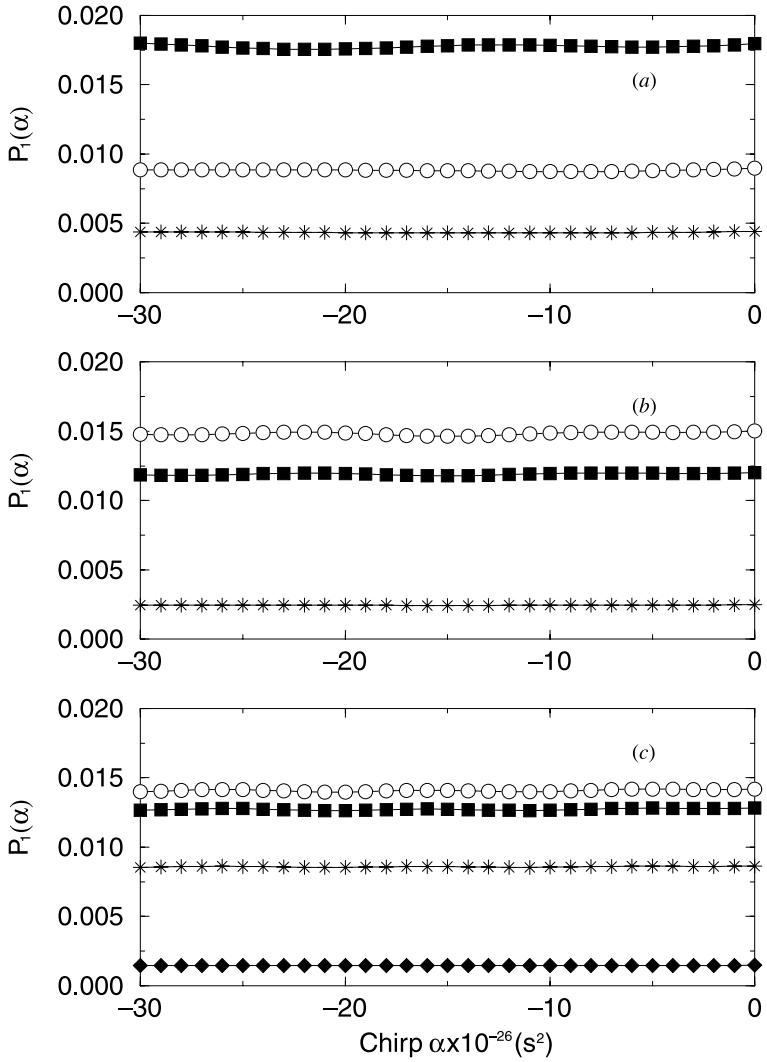

Figure 1. Populations of the first excited vibrational state as functions of the chirping parameter α with pulse duration $\tau_0 = 370$ fs, intensity $I_{max} = 10^{10}$ W cm^{-2} (unchirped) and different l, m initial states of $v = 0$. (*a*) Open circles, $l = 0$, $m = 0$; full squares, $l = 1$, $m = 0$; stars, $l = 1$, $m = 1$; (*b*) open circles, $l = 2$, $m = 0$; full squares, $l = 2$, $m = 1$; stars, $l = 2$, $m = 2$; (*c*) open circles, $l = 3$, $m = 0$; full squares, $l = 3$, $m = 1$; stars, $l = 3$, $m = 2$; full diamonds, $l = 3$, $m = 3$.

vibrational state, P_1 and P_3, for different initial states at intensity 10^{10} W cm^{-2}, shown in figures 1 and 2, respectively. Figure 1 has two notable features. First, P_1 is almost the same for all values of the chirping parameter α. This has been verified by experimental results [20] and theoretical calculations [12, 20]. The insensitivity regarding α is due to the fact that the pulse always has the opportunity to sweep across the $v = 0 \rightarrow 1$ transition for all α values. Secondly, for the states of the same v, l but different m, the populations are different and decrease as the azimuthal quantum number m increases. This is because the angular coupling part $d_{l',l} \equiv \langle Y_{l',m} | \cos\theta | Y_{l,m} \rangle$ decreases when the value of m increases. It is expected,

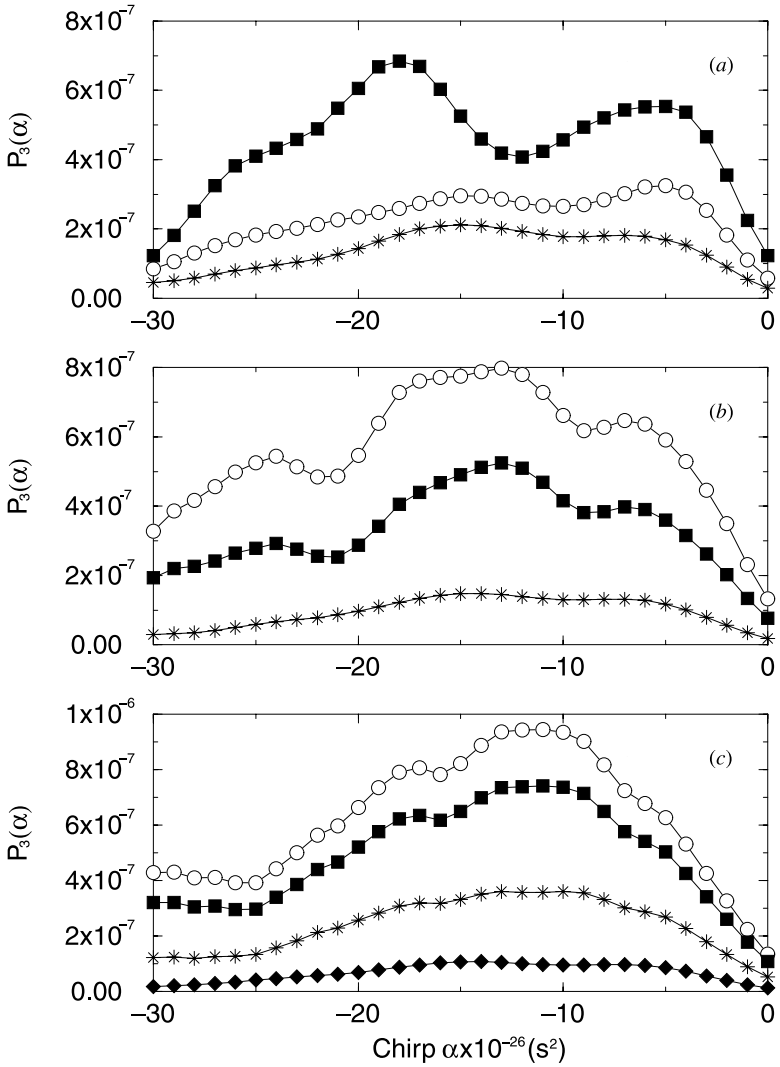

Figure 2. The third excited state populations P_3 against chirping parameter α at the end of the pulse. All the symbols and pulse parameters are the same as in figure 1.

intuitively, that the small m state has a larger density along the field polarization direction and is more more easily excited than large m states. This point was also confirmed by the strong field calculations of inert gas atoms in both the single-active-electron (SAE) model [39, 40] and *ab initio* time-dependent density functional theory (TDDFT) [41].

The P_3 population depicted in figure 2 uses the same parameters as in figure 1. We can see that the populations depend on the initial quantum number m and the population oscillation is more significant for small m than for large m. From the field-dressed three-level model, the interference pattern is determined by the excitation pathways from the initial state to the final state which are functions of intensity $I_{\max}$ and chirping α. The interference will disappear when the excitation is fully adiabatic or diabatic. This means that the diabatic (adiabatic) condition can be satisfied only when the frequency sweeping is very large (small) compared

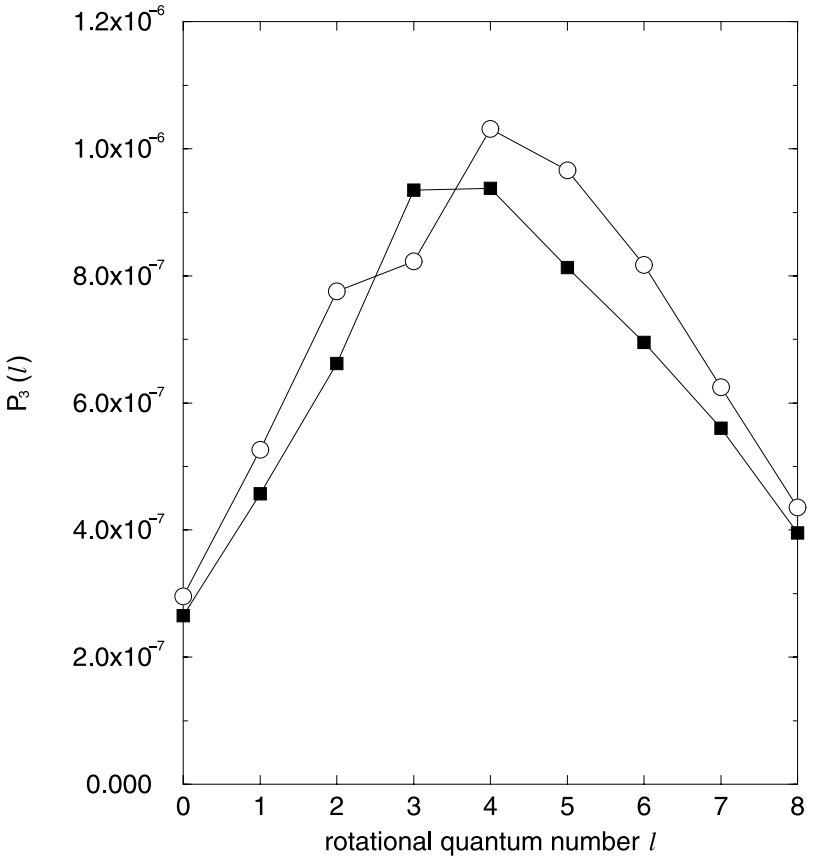

Figure 3. Populations P_3 as functions of the rotational quantum number l ($v = 0$, $m = 0$) of the initial states for pulse intensity $I_{\max} = 10^{10}$ W cm^{-2}, $\tau_0 = 370$ fs. Full squares, $\alpha = -1.0 \times 10^{-25}$ s^{-2}; open circles, $\alpha = -1.5 \times 10^{-25}$ s^{-2}.

with the Rabi frequency. For the experiments with Rb atoms and NO molecules [12, 17, 20], these two critical limits are not satisfied and we can see the oscillatory structure of populations against α. Although the Rb excitation has a clear oscillatory structure within a small range of values of α, the NO molecular experiment [20] demonstrated an unclear oscillation for α within -3×10^{-25} s^{-2}. The difference between chirping excitation for Rb atoms and NO molecules comes from:

(a) The $\alpha_{2\pi}$ oscillation period, π/A, where A is the area enclosed by the field-dressed three levels [17, 20], is larger for NO higher vibrational states than the Rb system. Therefore, in order to see the oscillation structure, we have to extend the chirping to large values as in figure 5 of [19].
(b) The Rb system is nearly a three-level system (5s, 5p and 5d), while there is a rotational manifold coupled with each vibrational state in NO which makes the transition more complicated than a simple three-level system and obscures the interference pattern.
(c) The transition moment of NO is smaller than the Rb transition moment by about one order of magnitude. The small NO transition moment leads to a weak excitation process which is more non-adiabatic than the Rb system and results in a vague population compared with Rb. The same reason can be applied to the oscillatory structure in figure 2 where the

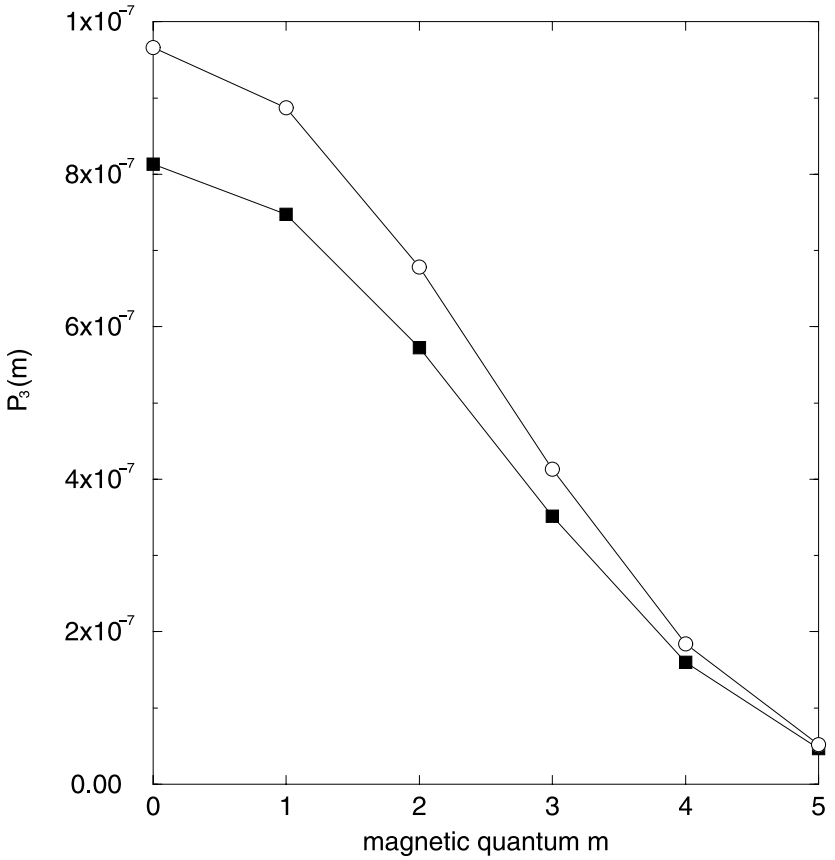

Figure 4. Populations P_3 *versus* azimuthal quantum number m ($\nu = 0$, $l = 5$) of the initial states. All the field parameters and symbols are the same as figure 3 except the initial states are different.

low-m initial states have significant oscillation populations but the high-m initial states result in smooth excitation populations. To sum up, the larger the transition moment is, the more sensitive the excitation population against the chirping parameter will be.

To give an idea of the role of initial states on excitation, figure 3 shows the P_3 population from different states $|\nu = 0, l = 0, \ldots, 8, m = 0\rangle$ with two different chirping parameters and $I_{\max} = 10^{10}$ W cm^{-2}. The most efficient initial states are located at around $l = 4$ and it is difficult to interpret why the excitation decreases for l greater than 4 in this complex process. It is possibly related to the fact that for high quantum numbers, l, the transition moment approaches a limiting value, i.e. $d_{l',l} \to 1$ as $l \to \infty$, and the intrapulse pump–dump mechanism becomes important as $l > 4$. Another possible cause is the interference due to different excitation routes that makes the population small for $l > 4$ at these specified chirping parameter values. We should note that figure 3 is for just two specific chirping parameters and there is insufficient evidence to assert that the best efficiency is achieved at around $l = 4$ according to the oscillation of populations versus α.

Figure 4 shows the P_3 populations of initial states $|\nu = 0, l = 5, m\rangle$ with $\alpha = -1.0 \times 10^{-25}$ and -1.5×10^{-25} s^{-2}. It is easy to understand the population decreases with increasing m due

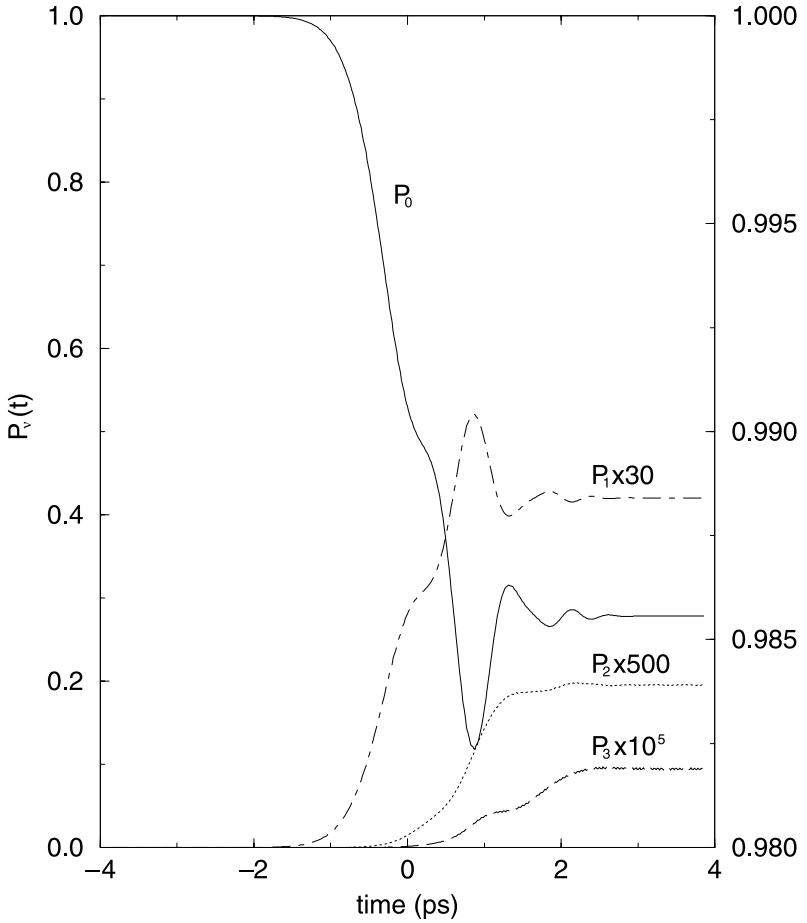

Figure 5. The time dependence of populations P_v, $v = 0, 1, 2, 3$ of initial state $|v = 0, l = 3, m = 0\rangle$ at $\alpha = -1.0 \times 10^{-25}$ s^{-2}, $\tau = 1.54$ ps and intensity $I_{\text{chirp}} = 2.4 \times 10^9$ W cm^{-2}.

to the small transition moment of large m, and the low-m states oriented along the polarization direction of the laser field are easily excited to high-vibrational states.

3.2. The thermal effect and the excitation process

As mentioned above, the intrapulse pump–dump may play an important role during the excitation process. It is worthwhile exploring this process in detail. First, in figure 5, we plot the populations P_v as functions of time which shows that the populations are excited sequentially by frequency decreasing order, $v = 0 \rightarrow 1$ at -1.5 ps, $v = 1 \rightarrow 2$ at -0.5 ps and $v = 2 \rightarrow 3$ at 0 ps (the pulse starts at about -4 ps). In the initial stages of the $v = 0, l = 3 \rightarrow v = 1$ transition, there is a population fluctuation, due to the Rabi oscillation, and a small fraction of the population comes from the dump to $v = 0, l = 1$ or 5. This can be seen from figure 6(*a*) where the population oscillations of $P_{1,4}$ and $P_{1,2}$ are clear and $P_{1,4}$ is populated earlier than $P_{1,2}$ since the chirping is from blue to red. Figure 6(*c*) shows the dump population for the $v = 1, l = 4 \rightarrow v = 0, l = 5$ and $v = 1, l = 2 \rightarrow v = 0, l = 1$ transitions after a 0.5 ps time

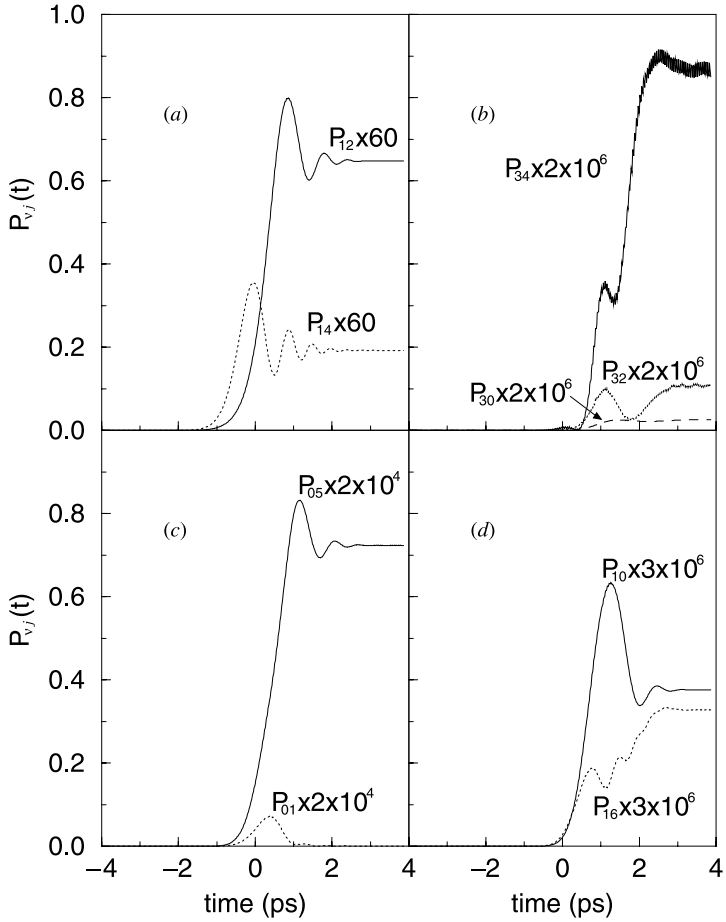

Figure 6. Populations $P_{v,l}$ $(m = 0)$ against time during chirping excitation with the same initial state and field parameters, E_m, τ and α, as in figure 5. (*a*) and (*b*) show the pump-process populations $|v = 0, l = 3\rangle \rightarrow |v = 1, l = 3 \pm 1\rangle$ and $|v = 2, l = 1, 3, 5\rangle \rightarrow |v = 3, l = 0, 2, 4, 6\rangle$ ($P_{3,6}$ is not shown), respectively. (*c*) shows the dump-process populations $|v = 1, l = 4\rangle \rightarrow |v = 0, l = 5\rangle$ and $|v = 1, l = 2\rangle \rightarrow |v = 0, l = 1\rangle$; while (*d*) presents the dump populations of the $|v = 2, l = 1\rangle \rightarrow |v = 1, l = 0\rangle$ and $|v = 2, l = 5\rangle \rightarrow |v = 1, l = 6\rangle$ transitions.

delay of the $v = 0 \rightarrow v = 1$ excitation. Mishima and Yamashita [8] demonstrated that the excitation population distribution will change from high vibrational states to lower vibrational states in two-vibronic potential energy curves (PECs) due to the intrapulse pump–dump process when the number of vibrational states in the ground electronic state changes from one to four. This pump–dump mechanism may inhibit the chirping excitation efficiency in addition to the excitation pathway interference although the dump populations are small in our calculation. The pump and dump histories of the $v = 2$ state are also plotted in figures 6(*b*) and (*d*) where the dump populations are of the same order of magnitude as the pump populations in contrast to the $v = 0 \longleftrightarrow v = 1$ transition.

As the transitions approach being fully adiabatic or diabatic, the interference will decrease. Therefore, it is interesting to study the effect of intensities on the population transfer. The adiabatic criterion $\mathrm{d}\omega/\mathrm{d}t \ll \Omega^2_{\mathrm{Rabi}}$ is not always satisfied by changing the parameter α, and

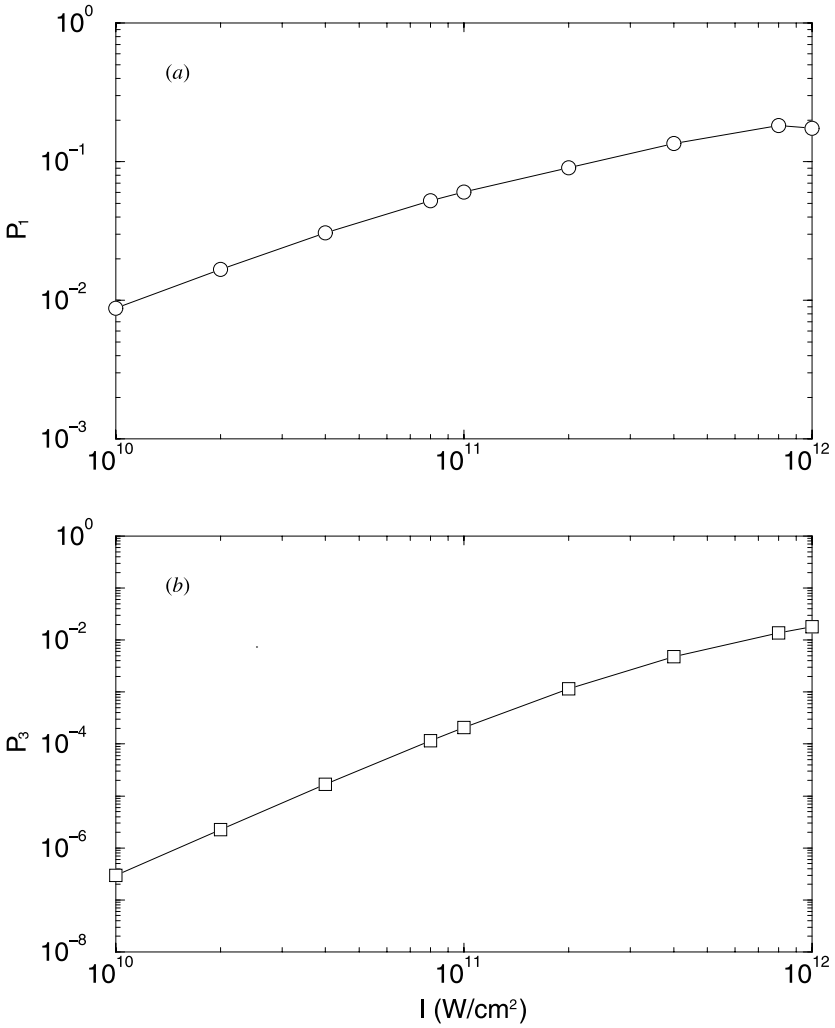

Figure 7. The intensity dependence of populations P_1 and P_3 of initial state $|v = 0, l = 0, m = 0\rangle$ for $\alpha = -1.5 \times 10^{-25}$ s^{-2}, $\tau = 2.28$ ps. Note that in (*b*) the population at $I_{max} = 10^{12}$ W cm^{-2} is about four orders of magnitude greater than the population at intensity $I_{max} = 10^{10}$ W cm^{-2}.

one of the plausible ways to control the excitation within the adiabatic regime is to increase the laser intensity. In our previous calculation [12], the adiabatic condition is not satisfied due to the low field intensity, and we therefore calculate the population transfer of P_1 and P_3 at different intensities to investigate the influence of E_m on population transfer. In figure 7 we can see that the P_1 population increases by one order of magnitude and that the P_3 population increases five orders of magnitude when the intensity increases by two orders of magnitude (E_m increases by one order of magnitude). This is a dramatic increase for high-vibrational-state excitation where the pulse improves the adiabatic condition significantly for high-vibrational states. However, the change in low vibrational states is limited because these states are excited at around maximum pulse intensity $\boldsymbol{E}(t = 0)$, while the high states excitation occurs around the pulse decay region.

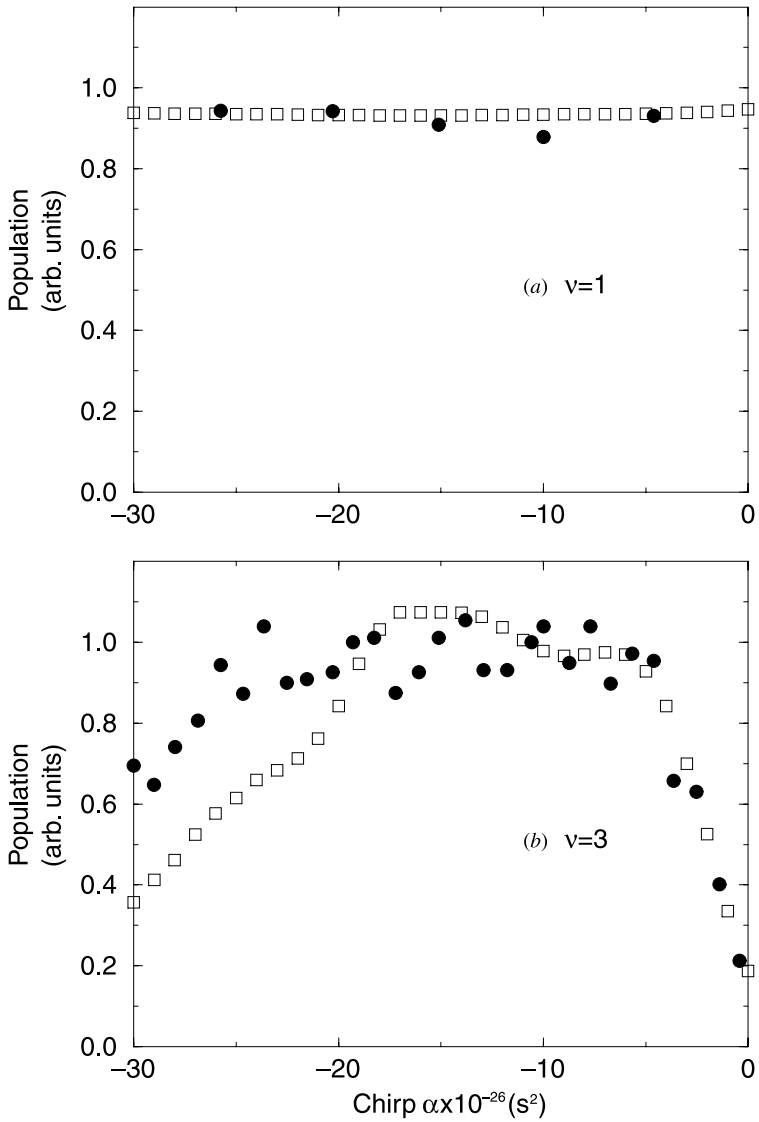

Figure 8. The populations P_1 and P_3 as functions of the chirping parameter α: full circles are the experimental data [19] and open squares are the calculated results of this work. The populations are averaged over the initial states shown in figures 1 and 2 according to the thermal distribution. The field intensity $I_{\max}$ is 10^{10} W cm^{-2} and the pulse duration $\tau_0 = 370$ fs.

Physically, the vibrational populations have to take into account the rotational thermal effect before the molecule interacts with the chirped pulse. Therefore, the final population for each specific vibrational state must be averaged over the rotational thermal distribution. In figure 8 the populations P_1 and P_3 are averaged over the thermal distribution of rotational states up to $l = 3$, $|m| = 3$ at $T = 15$ K. In figure 8(b) we can see that the two local maximum populations at $\alpha = -5 \times 10^{-26}$ and -1.5×10^{-25} s^{-2} are smoothed out in comparison with figure 3 in [12]. Furthermore, our calculation shows descending populations for α at around -3.0×10^{-25} s^{-2} in agreement with the experimental results [20] where

the numerical simulation with a few coupling states gives ascending populations at around $\alpha = -3.0 \times 10^{-25}$ s^{-2}. This implies that the pathway interference, as well as the thermal average, have to be considered in the population calculation.

4. Conclusions

We have examined the chirping excitation process of NO molecules and its limitation in detail. To reach efficient excitation, the frequency-sweeping rate must satisfy the adiabatic criterion $\mathrm{d}\omega/\mathrm{d}t \ll \Omega_{\mathrm{Rabi}}^2$ and the chirping interference pattern of population will disappear in the adiabatic limit. On the other hand, to cope with this criterion, one can increase the field intensity when the transition moment is small and the frequency-sweeping rate is finite. For a strong field the ionization process will dominate the dissociative one and the intrapulse pump–dump mechanism is no longer negligible. As a result, the dissociation of diatomic molecules in medium intensity will be limited by the interference pathways and the pump–dump mechanism. We have neglected the NO open-shell nature and its upper doublet state in the calculation. This could make the interference pathway simpler and their coupling different from the actual NO chirping excitation, and hence, the populations might be a little different from the experimental result. However, the calculations still provide useful insights into the chirped-pulse excitation dynamics.

When the field–matter interaction involves more than three atomic species, namely, the polyatomic molecular excitation and the laser-excitation collision [42–46], a full calculation is nearly impossible with present computational power. It is also difficult to describe such a complicated process in a simple analytical form, and then numerical TDSE is usually a necessary and feasible solution. Therefore, in order to understand the energy transfer and distribution, and relaxation processes due to the presence of collisions or the coupling of neighbour bondings in the chirping excitation of a specified molecular bond, an efficient, accurate and simple numerical approximation scheme is required [42, 43, 47]. It is our future goal to look for a suitable method to study the factors that influence the state-selective chirping excitation.

Acknowledgments

The authors acknowledge the National Science Council of Taiwan for financial support under the contract no NSC89-2112-M009-005. We are grateful to Professor Noordam for sending us the collected papers of the Femtophysics Group of AMOLF, Netherlands during this work. JTL is partially supported by the Computational Materials Research Program, NCTS, Taiwan.

References

[1] Gross P, Neuhauser D and Rabitz H 1992 *J. Chem. Phys.* **96** 2834
Kaluža M, Muckerman J T, Gross P and Rabitz H 1994 *J. Chem. Phys.* **100** 4211
[2] Chelkowski S, Bandrauk A D and Corkum P B 1990 *Phys. Rev. Lett.* **65** 2355
[3] Chelkowski S and Bandrauk A D 1990 *Phys. Rev.* A **41** 6480
Chelkowski S and Bandrauk A D 1991 *Chem. Phys. Lett.* **186** 264
[4] Chelkowski S and Bandrauk A D 1993 *J. Chem. Phys.* **99** 4297
[5] Just B, Manz J and Trisca I 1992 *Chem. Phys. Lett.* **193** 423
Just B, Manz J and Paramonov G K 1992 *Chem. Phys. Lett.* **193** 429
[6] Melinger J S, McMorrow D, Hillegas C and Warren W S 1995 *Phys. Rev.* A **51** 3366
[7] Guérin S 1997 *Phys. Rev.* A **56** 1458
[8] Mishima K and Yamashita K 1998 *J. Chem. Phys.* **109** 1801

[9] Mishima K, Hayashi M, Lin J T, Yamashita K and Lin S H 1999 *Chem. Phys. Lett.* **309** 279
[10] Mishima K and Yamashita K 1999 *J. Chem. Phys.* **110** 7756
[11] Lin J T, Chuu D S and Jiang T F 1998 *Phys. Rev.* A **58** 2337
[12] Lin J T, Hayashi M, Lin S H and Jiang T F 1999 *Phys. Rev.* A **60** 3911
[13] Lin J T, Lai T L, Chuu D S and Jiang T F 1998 *J. Phys. B: At. Mol. Opt. Phys.* **31** L117
[14] Lin J T and Jiang T F 1999 *J. Phys. B: At. Mol. Opt. Phys.* **32** 4001
[15] Liu W K, Wu B and Yuan J M 1995 *Phys. Rev. Lett.* **75** 1292
[16] Yuan J M and Liu W K 1998 *Phys. Rev.* A **57** 1992
[17] Balling P, Maas D J and Noordam L D 1994 *Phys. Rev.* A **50** 4267
[18] Vrijen R B, Lankhuijzen G M, Maas D J and Noordam L D 1996 *Comment. At. Mol. Phys.* **33** 67–82
[19] Maas D J, Duncan D I, Vrijen R B, van der Zande W J and Noordam L D 1998 *Chem. Phys. Lett.* **290** 75
[20] Maas D J, Vrakking M J J and Noordam L D 1999 *Phys. Rev.* A **60** 1351
[21] Maas D J, Rella C W, Antoine P, Toma E S and Noordam L D 1999 *Phys. Rev.* A **59** 1374
[22] Cao J, Bardeen C J and Wilson K R 1998 *Phys. Rev. Lett.* **80** 1406
[23] Kleiman V D, Arrivo S M, Melinger J S and Heilweil E J 1998 *Chem. Phys.* **233** 207
[24] Meyer S, Meier C and Engel V 1998 *J. Chem. Phys.* **108** 7631
[25] Shi S and Rabitz H 1989 *Chem. Phys.* **139** 185
Shi S and Rabitz H 1990 *J. Chem. Phys.* **92** 364
[26] Krempl S, Eisenhammer T, Hübler A, Mayer-Kress G and Milonni P W 1992 *Phys. Rev. Lett.* **69** 430
[27] Chelkowski S and Bandrauk A D 1992 *Coherence Phenomena in Atoms and Molecules in Laser Fields (NATO ASI series, Series B)* ed A D Bandrauk (New York: Plenum) **287** 333
[28] Guldberg A and Billing G D 1991 *Chem. Phys. Lett.* **193** 229
[29] Bloembergen N and Zewail A H 1984 *J. Chem. Phys.* **88** 5459
[30] Korolkov M V, Paramonov G K and Schmidt B 1996 *J. Chem. Phys.* **105** 1862
[31] Andrianov I V and Paramonov G K 1999 *Phys. Rev.* A **59** 2134
[32] Tsukada N, Nomura Y and Isu T 1999 *Phys. Rev.* A **59** 2852
[33] Melinger J S, Gandhi S R, Hariharan A, Goswami D and Warren W S 1994 *J. Chem. Phys.* **101** 6439
[34] Treacy E B 1969 *IEEE J. Quantum Electron.* **5** 454
[35] Billingsley F P II 1975 *J. Chem. Phys.* **62** 864
[36] Siegman A E 1986 *Lasers* (Mill Valley, CA: University Science Books)
[37] Feit M D, Fleck J A Jr and Steiger A 1982 *J. Comput. Phys.* **47** 412
[38] Feit M D and Fleck J A Jr 1984 *J. Chem. Phys.* **80** 2578
[39] Kulander K C 1987 *Phys. Rev.* A **35** 445
[40] Kulander K C and Shore B W 1990 *J. Opt. Soc. Am.* B **7** 502
[41] Ullrich C A and Gross E K U 1997 *Comment. At. Mol. Phys.* **33** 311
[42] Ermoshin V A, Kazansky A K and Engel V 1999 *Chem. Phys. Lett.* **302** 20
[43] Ermoshin V A, Kazansky A K and Engel V 1999 *J. Chem. Phys.* **111** 7807
[44] Liu Q, Wan C and Zewail A H 1996 *J. Phys. C: Solid State Phys.* **100** 18 666
[45] Chelkowski S and Bandrauk A D 1991 *Chem. Phys. Lett.* **186** 264
[46] Dion C M, Bandrauk A D, Atabek A, Keller A, Umeda H and Fu Y 1999 *Chem. Phys. Lett.* **302** 215
[47] Nettesheim P, Bornemann F A, Schmidt B and Schütte C 1996 *Chem. Phys. Lett.* **256** 581